

Polarimetric parameters associated to commercial optical fibers

O. J. Velarde-Escobar^a, K. M. Salas-Alcántara^b, R. Espinosa-Luna^{b,*}, G. Atondo-Rubio^a, and I. Torres-Gómez^c

^aGIPYS, Posgrado en Física, Facultad de Ciencias Físico-Matemáticas, Universidad Autónoma de Sinaloa, Ciudad Universitaria s/n, 80010 Culiacán, Sinaloa, México,

e-mail: osvel@uas.edu.mx; gatondo@uas.edu.mx

^bGIPYS, Centro de Investigaciones en Óptica, A. C., Loma del Bosque 115,

Colonia Lomas del Campestre, 37150 León, Guanajuato, México,

e-mail: alrak@cio.mx; *reluna@cio.mx

^cCentro de Investigaciones en Óptica, A. C., Loma del Bosque 115,

Colonia Lomas del Campestre, 37150 León, Guanajuato, México,

e-mail: itorres@cio.mx

Received 20 May 2014; accepted 11 September 2014

The most important polarimetric parameters are determined for six different types of commercially available optical fibers, at 1550 nm of transmission wavelength. The diattenuation, polarizance, retardance, polarization dependent loss (PDL), among other conventional polarimetric parameters, are determined from the Mueller matrix associated to 1m length of each fiber studied here. An improvement to the data analysis method, reported recently by our group, is presented. Results obtained show the fibers can be used not only as static elements, but also as versatile optical devices, depending on the incident polarization state employed.

Keywords: Polarization in optical fibers; birefringence in optical fiber; analysis of polarized light.

Se determinan los parámetros polarimétricos más importantes para seis distintos tipos de fibras ópticas accesibles comercialmente, a una longitud de onda de transmisión de 1550 nm. La diatenuación, polarizancia, retardancia, pérdidas dependientes de la polarización (PDL), entre otros parámetros polarimétricos convencionales, se obtienen mediante las matrices de Mueller asociadas a 1 m de longitud de cada fibra estudiada aquí. Una mejora al método de análisis de datos, reportado recientemente por nuestro grupo, es presentada. Los resultados obtenidos muestran que las fibras no solo pueden utilizarse como elementos ópticos estáticos, sino como dispositivos versátiles, dependiendo del estado de polarización incidente.

Descriptores: Polarización en fibras ópticas; birrefringencia en fibras ópticas; análisis de luz polarizada.

PACS: 42.81.Gs; 78.20.Fm

1. Introduction

The use of optical fibers in communications as the transmission medium or in applications as sensors in medical, engineering, and scientific fields is a common theme nowadays [1-4]. It is well known an optical fiber can be used as a single- or as a multi-mode transmission medium, depending on the operation wavelength employed, core-cladding diameter ratio, and its numerical aperture [5]. The single- or mono-mode operation in optical fibers (SMF) is particularly important due to the use in long distance transmission range because there is a need to transmit signals which, by their nature, cannot be transmitted simultaneously without elaborate means to aid signal recovery. A solution to this problem is to transmit the signals at different wavelengths which require wavelength multiplexing and demultiplexing arrangements at the transmitting and receiving ends of the link, respectively. With the trend towards ever increasing bit rates, there is a requirement for wavelength multiplexing and demultiplexing methods which are compatible with single-mode optical fiber links. Methods of wavelength demultiplexing, which are currently available in single-mode systems, employ either interference filters or gratings or directional couplers or a combination of these, where they exhibit low signal dis-

persion (low loss in transmitted intensity). Multimode fibers (MMFs) are preferred for home and business, because they are easy to connect, need low-precision components, and permit wavelength-multiplexing.

Single-mode fibers with typical core radii less than 10 μm permit transfer rates of 10 Gb/sec. One of the main potential applications of single-mode optical fibers is their use in encrypted optical and quantum communications, where the polarimetric properties are essential elements to determine their applications in this emerging area [6]. Properties such as the polarization dependent loss, the birefringence, the anisotropic depolarization degree, among others, represent valuable information for a lot of possible applications like the transmission of entangled pair of photons to long distances using single-mode fibers [6]. In this sense, the Mueller-Stokes matrix formalism, provides an easy and direct way to get the polarimetric properties when the depolarization scalar metrics are applied to the Mueller matrix [7-10].

In this work, the Mueller matrices associated to six different commercial optical fibers are obtained and several depolarization scalar metrics are employed to analyze each one of them.

TABLE I. Polarization-dependent parameters derived from the Mueller matrix.

Depolarization index, $DI(M)$.	$0 \leq DI(M) = \left\{ \sum_{j,k=0}^3 m_{jk}^2 - m_{00}^2 \right\}^{1/2} / \sqrt{3} m_{00} \leq 1$
Degree of polarization, $DoP(M, S)$.	$0 \leq DoP(M, S) = \frac{\sqrt{(s_1^0)^2 + (s_2^0)^2 + (s_3^0)^2}}{s_0^0}$ $= \frac{\left[\sum_{j=1}^3 (m_{j0}s_0^i + m_{j1}s_1^i + m_{j2}s_2^i + m_{j3}s_3^i) \right]^2}{m_{00}s_0^i + m_{01}s_1^i + m_{02}s_2^i + m_{03}s_3^i}}{1/2} \leq 1$
Anisotropic degree of depolarization, Add .	$0 \leq Add = \frac{(DoP)_{Max}^0 - (DoP)_{min}^0}{(DoP)_{Max}^0 + (DoP)_{min}^0} \leq 1$
Total diattenuation, $D(M)$.	$0 \leq D(M) = \sqrt{m_{01}^2 + m_{02}^2 + m_{03}^2} / m_{00} \leq 1$
Linear diattenuation, LD .	$0 \leq LD(M) = \sqrt{m_{01}^2 + m_{02}^2} / m_{00} \leq 1$
Circular diattenuation, CD .	$0 \leq CD(M) = \sqrt{m_{03}^2} / m_{00} \leq 1$
Total polarizance, $P(M)$.	$0 \leq P(M) = \sqrt{m_{10}^2 + m_{20}^2 + m_{30}^2} / m_{00} \leq 1$
Linear polarizance, LP .	$0 \leq LP(M) = \sqrt{m_{10}^2 + m_{20}^2} / m_{00} \leq 1$
Circular polarizance, CP .	$0 \leq CP(M) = \sqrt{m_{30}^2} / m_{00} \leq 1$
Q(M) metric, $Q(M)$.	$0 \leq Q(M) = \frac{\sum_{j=1,k=0}^3 m_{jk}^2}{\sum_{k=0}^3 m_{0k}^2} = \frac{3[DI(M)]^2 - [D(M)]^2}{1 + [D(M)]^2}$ $= \frac{\{\sum_{j,k=1}^3 m_{jk}^2\} / m_{00}^2 + [P(M)]^2}{1 + [D(M)]^2} \leq 3$
Gil-Bernabeu theorem, TGB .	$Tr(M^t M) = 4m_{00}^2$
Polarization dependent loss, PDL .	$PDL = 10 \log(T \max / T \min) = 10 \log \left[\frac{m_{00} + (m_{01}^2 + m_{02}^2 + m_{03}^2)^{1/2}}{m_{00} - (m_{01}^2 + m_{02}^2 + m_{03}^2)^{1/2}} \right]$
Gain, g .	$0 \leq g = \frac{s_0^o}{s_0^i} = \frac{m_{00}s_0^i + m_{01}s_1^i + m_{02}s_2^i + m_{03}s_3^i}{s_0^i} \leq 1$
Total retardance, R .	$R = \cos^{-1} \left(\frac{1}{2} Tr(M_R) - 1 \right)$
Linear retardance, δ .	$\delta = \cos^{-1} \left(\sqrt{[M_R(1,1) + M_R(2,2)]^2 + [M_R(2,1) - M_R(1,2)]^2} - 1 \right)$
Circular retardance, Cr .	$Cr = \frac{1}{2} \tan^{-1} \left\{ \frac{M_R(2,1) - M_R(1,2)}{M_R(1,1) + M_R(2,2)} \right\}$

The polarizance and the diattenuance parameters (linear, circular, and total), the degree of polarization, the depolarization index, the Q(M) metric, the Gil-Bernabeu theorem, the polarization dependent loss, the anisotropic depolarization degree, and the retardances (linear, circular, and total) are calculated from the Mueller matrix [7-15]. An improvement to a reported method by our group [8] is presented for the data analysis. Results show the optical fibers can also be used as devices, whose optical responses are clearly dependent on the incident polarization state.

2. Mathematical Mueller-Stokes formalism

The linear response of a medium to the polarization intensity, characterized by a Mueller matrix M, is given by [11]

$$s^o = MS^i \Rightarrow \begin{pmatrix} S_0^o \\ S_1^o \\ S_2^o \\ S_3^o \end{pmatrix} = \begin{pmatrix} m_{00} & m_{01} & m_{02} & m_{03} \\ m_{10} & m_{11} & m_{12} & m_{13} \\ m_{20} & m_{21} & m_{22} & m_{23} \\ m_{30} & m_{31} & m_{32} & m_{33} \end{pmatrix} \times \begin{pmatrix} S_0^i \\ S_1^i \\ S_2^i \\ S_3^i \end{pmatrix} = \begin{pmatrix} m_{00}S_0^i + m_{01}S_1^i + m_{02}S_2^i + m_{03}S_3^i \\ m_{10}S_0^i + m_{11}S_1^i + m_{12}S_2^i + m_{13}S_3^i \\ m_{20}S_0^i + m_{21}S_1^i + m_{22}S_2^i + m_{23}S_3^i \\ m_{30}S_0^i + m_{31}S_1^i + m_{32}S_2^i + m_{33}S_3^i \end{pmatrix} \quad (1)$$

where S is named the Stokes vector. $S^{i,o}$ represents the polarization state of the incident and the output light beams, respectively, defined in terms of the orthogonal components of the electric field vector (E_p, E_s) and their phase differences.

The normalized polarized Stokes parameters can be displayed in a real three dimensional space as a function of the azimuth ($0 \leq 2\psi \leq \pi/2$) and the ellipticity ($-\pi/2 \leq 2\varepsilon \leq \pi/2$) angles of the Poincaré sphere, respectively [11].

$$S = s_0 DoP \begin{pmatrix} 1 \\ \cos(2\varepsilon) \cos(2\psi) \\ \cos(2\varepsilon) \sin(2\psi) \\ \sin(2\varepsilon) \end{pmatrix}, \quad (2)$$

where s_0 represents the average light intensity associated to the Stokes parameters and DoP is the degree of polarization.

By applying the depolarization scalar metrics (see Table I) to the Mueller matrix M , it is possible to analyze the polarimetric properties associated to a section of the optical fibers and their capability to depolarize light [7-15]. One can observe that all of them are obtained from the Mueller matrix directly

Where M_R is the Mueller matrix associated to the retardance contribution, obtained from the polar decomposition method [12].

3. Experimental determination of the Mueller matrix

In order to experimentally determine the Mueller matrix elements of the optical fibers, we propose to use the method of six measurements reported recently by our group, where a set of six incident Stokes vectors are used and analyzed [8]. The incident and the analyzed Stokes vectors correspond to linear polarization states parallel (**p**), perpendicular (**s**), to **+45** degrees (**+**), and to **-45** degrees (**-**), and to circular right- (**r**) and left-hand (**l**) polarization states, respectively. In a recent work, our group has reported the Mueller matrix parameters can be obtained by applying the following equations (see Ref. 8), named there as Eqs. (6):

$$\begin{aligned} m_{00} &= \frac{1}{2} (s_0^{pd} + s_0^{sd}), & m_{01} &= \frac{1}{2} (s_0^{pd} - s_0^{sd}), & m_{02} &= \frac{1}{2} (s_0^{+d} - s_0^{-d}), & m_{03} &= \frac{1}{2} (s_0^{rd} - s_0^{ld}), \\ m_{10} &= \frac{1}{2} (s_1^{pd} s_0^{pd} + s_1^{sd} s_0^{sd}), & m_{11} &= \frac{1}{2} (s_1^{pd} s_0^{pd} - s_1^{sd} s_0^{sd}), & m_{12} &= \frac{1}{2} (s_1^{+d} s_0^{+d} - s_1^{-d} s_0^{-d}), & m_{13} &= \frac{1}{2} (s_1^{rd} s_0^{rd} - s_1^{ld} s_0^{ld}), \\ m_{20} &= \frac{1}{2} (s_2^{pd} s_0^{pd} + s_2^{sd} s_0^{sd}), & m_{21} &= \frac{1}{2} (s_2^{pd} s_0^{pd} - s_2^{sd} s_0^{sd}), & m_{22} &= \frac{1}{2} (s_2^{+d} s_0^{+d} - s_2^{-d} s_0^{-d}), & m_{23} &= \frac{1}{2} (s_2^{rd} s_0^{rd} - s_2^{ld} s_0^{ld}), \\ m_{30} &= \frac{1}{2} (s_3^{pd} s_0^{pd} + s_3^{sd} s_0^{sd}), & m_{31} &= \frac{1}{2} (s_3^{pd} s_0^{pd} - s_3^{sd} s_0^{sd}), & m_{32} &= \frac{1}{2} (s_3^{+d} s_0^{+d} - s_3^{-d} s_0^{-d}), & m_{33} &= \frac{1}{2} (s_3^{rd} s_0^{rd} - s_3^{ld} s_0^{ld}), \end{aligned}$$

We have improved these relationships, by considering a multiplicative factor associated with the degree of polarization, which now has been incorporated to each detected Stokes parameter, with exception to elements of the first row, which are detected directly as associated to the normalized power registered by the commercial equipment (this factor is reduced to the unitary value when the system under study does not depolarize). By following a similar development than the described in Ref. 8, but now taking into account that the equipment provides the Stokes vectors of the polarized part of the detected light, the following improved equations are obtained

$$\begin{aligned} m_{00} &= \frac{1}{2} (s_0^{pd} + s_0^{sd}), & m_{01} &= \frac{1}{2} (s_0^{pd} - s_0^{sd}), & m_{02} &= \frac{1}{2} (s_0^{+d} - s_0^{-d}), & m_{03} &= \frac{1}{2} (s_0^{rd} - s_0^{ld}), \\ m_{10} &= \frac{1}{2} (s_1^{pd} s_0^{pd} \rho^{pd} + s_1^{sd} s_0^{sd} \rho^{sd}), & m_{11} &= \frac{1}{2} (s_1^{pd} s_0^{pd} \rho^{pd} - s_1^{sd} s_0^{sd} \rho^{sd}), \\ m_{12} &= \frac{1}{2} (s_1^{+d} s_0^{+d} \rho^{+d} - s_1^{-d} s_0^{-d} \rho^{-d}), & m_{13} &= \frac{1}{2} (s_1^{rd} s_0^{rd} \rho^{rd} - s_1^{ld} s_0^{ld} \rho^{ld}), \\ m_{20} &= \frac{1}{2} (s_2^{pd} s_0^{pd} \rho^{pd} + s_2^{sd} s_0^{sd} \rho^{sd}), & m_{21} &= \frac{1}{2} (s_2^{pd} s_0^{pd} \rho^{pd} - s_2^{sd} s_0^{sd} \rho^{sd}), \\ m_{22} &= \frac{1}{2} (s_2^{+d} s_0^{+d} \rho^{+d} - s_2^{-d} s_0^{-d} \rho^{-d}), & m_{23} &= \frac{1}{2} (s_2^{rd} s_0^{rd} \rho^{rd} - s_2^{ld} s_0^{ld} \rho^{ld}), \\ m_{30} &= \frac{1}{2} (s_3^{pd} s_0^{pd} \rho^{pd} + s_3^{sd} s_0^{sd} \rho^{sd}), & m_{31} &= \frac{1}{2} (s_3^{pd} s_0^{pd} \rho^{pd} - s_3^{sd} s_0^{sd} \rho^{sd}), \\ m_{32} &= \frac{1}{2} (s_3^{+d} s_0^{+d} \rho^{+d} - s_3^{-d} s_0^{-d} \rho^{-d}), & m_{33} &= \frac{1}{2} (s_3^{rd} s_0^{rd} \rho^{rd} - s_3^{ld} s_0^{ld} \rho^{ld}), \end{aligned} \quad (3)$$

Where ρ^{kd} is the degree of polarization associated to the detected Stokes vector (S^{kd}), k stands for the polarization states ($k = p, s, \pm 45, r, \text{ and } l$) and d indicates “detected”. Equations (3) can be understood easily by taking into account the commercial software registers the total energy detected as the power, in normalized units, which is the origin of the “incomplete” term associated to this Stokesmeter system. However, it can be a “complete” Stokesmeter if the user multiplies the power detected

for each polarization, $(S_0^{p,s,+,-,r,l,d})$, by the normalized values detected for the remaining three Stokes parameters and for their corresponding degree of polarization factors, $(S_{1,2,3}^{p,s,+,-,r,l,d} S_0^{p,s,+,-,r,l,d} \rho^{p,s,+,-,r,l,d})$, this must be done for each polarization. This procedure sure will be easy to use once the manual of the system be consulted (it can be downloaded freely from the Thorlabs web site). Experience has shown us, indeed, it is true.

The six optical fiber studied here are commercially available (their technical characteristics are easily obtained by using any internet search engine). They have been selected just because are broadly employed in several laboratories and in the communications industry; in this way, our results could be of some interest for their users. Here are described only some basic characteristics, as reporter by their manufacturing company.

The optical fiber ESM-12-01 (fiber *a*), is an endlessly single-mode photonic crystal fiber (SM-PCF) used in sensors and modal interferometric applications mainly, it has an attenuation as low as < 0.8 dB/km for $\lambda = 1550$ nm. The fiber *b* is a Nufern's 980 nm (980 HP), which is described as high performance selected cut-off single-mode fiber (SMF), optimized for use by component manufacturers in the telecommunications industry. Fiber *b* offers exceptional uniformity

and core/clad concentricity specifications, very tight second mode cut-off tolerances, and tighter bend radius applications in miniaturized fiber optic packages. The optical fiber FS-PM-6621 (fiber *c*) is described as a polarization maintaining single mode fiber (SM-PMF), has a stress-induced birefringence which allows low loss transmission of polarized light with little cross talk between fiber polarization modes, and has an attenuation of 2 dB/km; these data were determined at 1300 nm. The SMF-28 (fiber *d*) is a Corning single mode fiber (SMF) and it has been widespread used in a long haul and regional networks, with a maximum attenuation of 0.17 dB/km. The LB 1300 (fiber *e*) is a low-birefringence fiber that preserves both linear and circular polarization and can relay with minimum error over large distances, with an attenuation of 4 dB/km. The optical fiber LB1300 present stress-induced birefringence and allows low loss transmission of polarized light with little cross talk between fiber polarization modes. It shows a SMF behavior at 1550 nm. The UV photosensitive fiber (fiber *f*) is used for grating fabrication and transmits light as a SMF at 1550 nm. Figure 1 shows the transversal sections of the optical fibers studied here, as observed by an optical microscope with amplification of 40X.

Each one of the fibers studied here had approximately one meter length and PC/FC connectors were employed to connect them with the equipment.

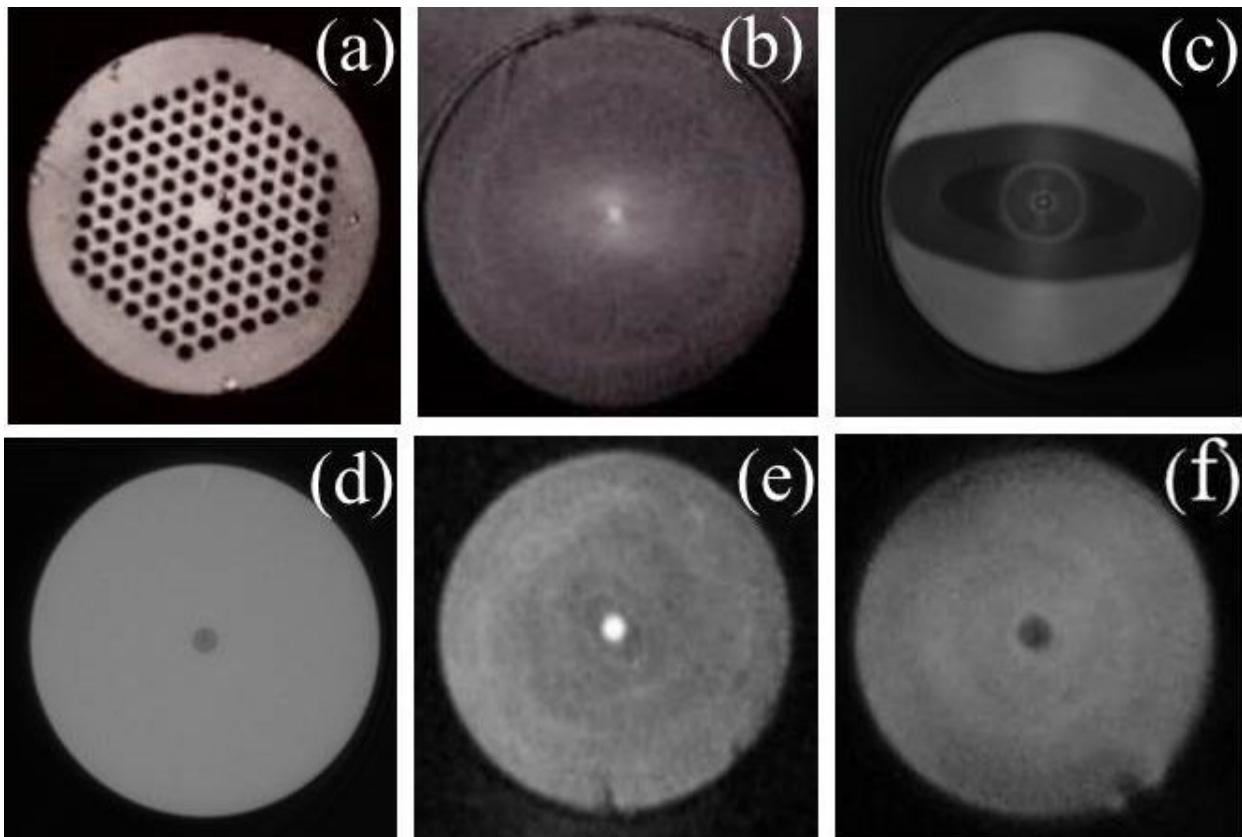


FIGURE 1. Transversal optical-microscopy sections of the commercial fibers a) ESM 12-01, b) 980 HP, c) FS-PM-6621, d) SMF-28, e) LB-300, and f) UV photosensitive fiber.

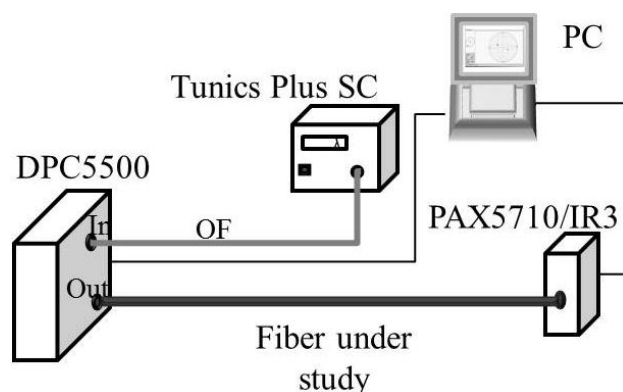


FIGURE 2. Diagram of the experimental setup employed for the determination of the Mueller matrix of the fibers.

4. Experimental results and discussion

The objective in this work is the analysis of the polarimetric properties associated to the former six commercial optical fibers, once the full determination of the Mueller matrix is obtained. The experimental setup sketched in Fig. 2 is used for the basic measurements of polarization properties of the optical fibers [8].

The light source is a tunable laser within 1450-1590 nm range (Anritsu, Tunics Plus SC), tuned to 1550 nm in this work. This laser is connected to a Deterministic Polarization Controller input, DPC, (Thorlabs, model DPC5500). The optical signal with arbitrary input polarization state enters on the DPC, while at its output we obtain a signal with a fixed and predetermined polarization state. The output signal from the DPC is used as a polarization state generator, PSG, for the fiber being studied, which is connected directly to the polarizer state analyzer, PSA, (Thorlabs, model PAX5710/IR3) and the measurements are taken for the six incident polarization states p , s , $+45$, -45 , r , and l , respectively. A computer controls the PSG and the PSA, and a computer program provides the calculus of the Mueller matrix, using the Stokes vectors measured. For each polarization state generated, the polarimeter analyzes the Stokes vector of the light beam leaving the system under study. Then, six measurements provide the 16 Mueller parameters required, according to the improved Eqs. (3). Once the Mueller matrices are determined for each fiber, their polarimetric parameters are

calculated, according to the relationships shown in Table I. The results obtained are shown in Table II.

The data shown in Table II represent the average linear response of the optical fibers to any linear, circular or elliptical incident polarization states, even when only six different polarization states have been used for the incidence. Observe that the data have been ordered according to the optical fibers' depolarization capability, where the first two scalar metrics (theorem of Gil-Bernabeu, TGB, and depolarization index, DI(M)) indicate the optical fibers depolarize the transmitted light (a unitary value means the fibers do not depolarize and can be described by the Jones formalism). Q(M) is consistent with them and shows the fibers are diattenuating also. The Add metric shows all the optical fibers depolarize anisotropically, this means some transmitted polarizations states are less affected than others. Fiber c shows a lower PDL value, which is consistent with the total diattenuation parameter, D(M). On the other hand, fiber d has the higher total polarizance value, which means it has a great capacity to polarize the transmitted light. The retardance parameter, R, shows all the fibers are birefringent. The reader can use any of these fibers according to his/her polarimetric requirements, or to apply a similar procedure to determine the specific response of his/her own fibers. This analysis does not provide information about a particular transmitted (or incident) polarization state, only shows the average optical response to any polarization state. However, considering that the anisotropic depolarization degree, Add, provides information related with the anisotropic response of the fiber to the polarization state transmitted, the output degree of polarization can provide specific information about any particular state. Figure 3 shows the graphical representation of the output degree of polarization, DoP, as a function of the incident polarization states for the six optical fibers.

Observe the DoP output is different for each optical fiber, which means they can be used not only as static elements, but also as dynamic devices, whose response can be modulated depending on the selected incident polarization state (represented in the basal plane as the azimuth, ψ , and the ellipticity, ϵ , angles, see Eq. (2)). Observe that some DoP output values are outside the physical realizable limits for some possible incident polarization states (for all the incident polarization states used here, always physically realizable values were ob-

TABLE II. Polarimetric data obtained from the Mueller matrices associated to the optical fibers studied.

Fiber	TGB	DI(M)	Q(M)	Add	PDL	D(M)	LD	CD	P(M)	LP	CP	R	Cr	δ
a	0.826	0.877	2.170	0.170	4.225	0.208	0.061	0.199	0.839	0.829	0.126	1.256	0.146	1.226
b	0.647	0.728	1.059	0.534	11.177	0.507	0.507	0.017	0.505	0.430	0.265	1.607	-0.334	2.294
c	0.621	0.704	1.474	0.311	1.397	0.07	0.064	0.027	0.592	0.587	0.071	1.571	0.050	2.674
d	0.601	0.684	1.357	0.112	2.903	0.144	0.099	0.105	0.928	0.661	0.651	2.508	0.348	0.831
e	0.580	0.664	1.256	0.415	3.505	0.174	0.157	0.074	0.469	0.426	0.195	1.769	-0.727	0.608
f	0.370	0.400	0.452	0.536	2.852	0.142	0.135	0.042	0.189	0.024	0.188	2.231	0.716	10135

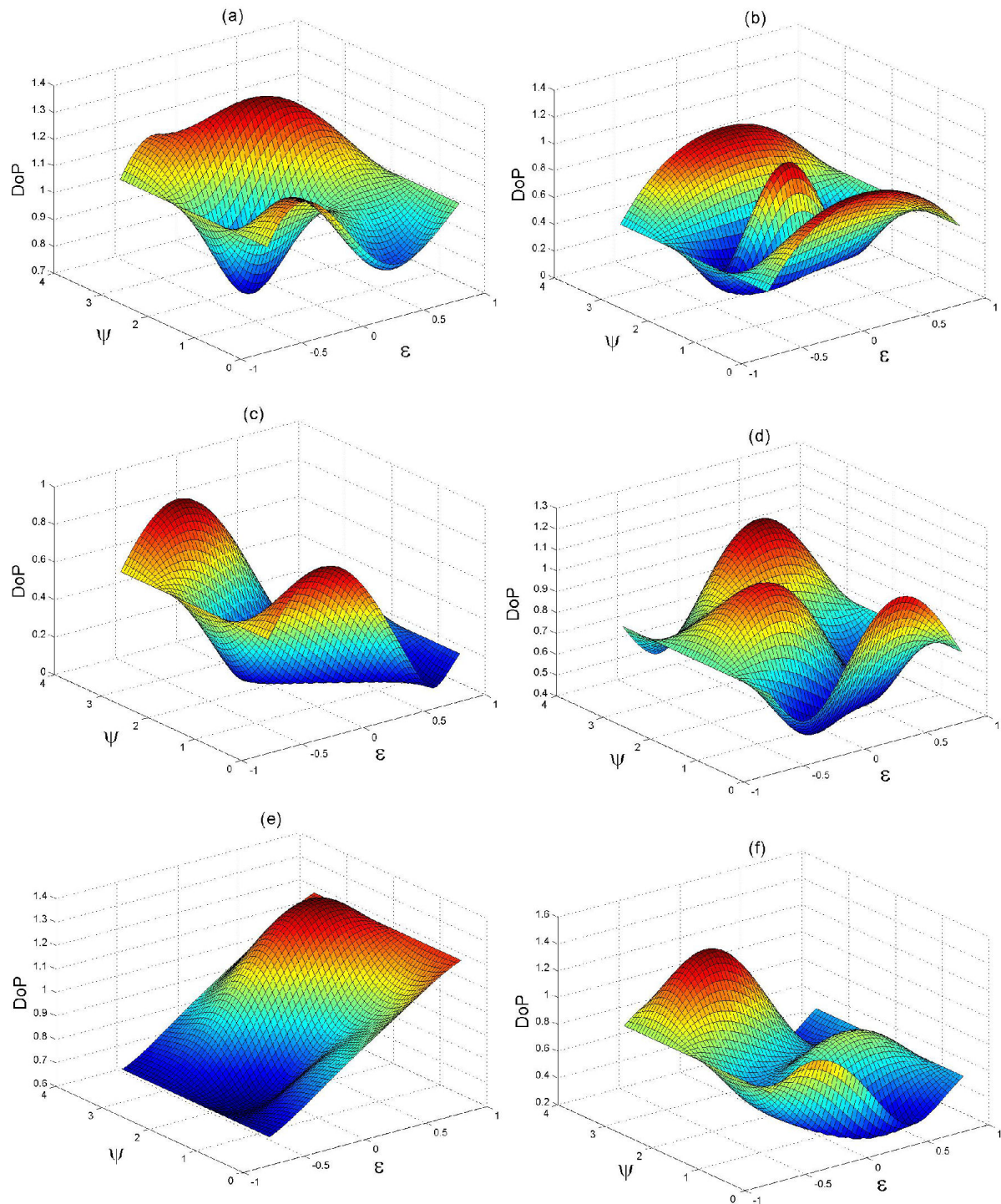


FIGURE 3. Output degree of polarization versus the azimuthal (ψ) and the ellipticity (ϵ) angles, for fibers a (Fig. 3.a), b (Fig. 3.b), c (Fig. 3.c), d, (Fig. 3.d), e (Fig. 3.e), and f (Fig. 3.f).

tained). A possible explanation for this behavior can be associated to the calibration procedure available with the commercial equipment employed here. The calibration of the experimental arrangement, ideally should be done with the use of a truly non-depolarizing, polarization-maintaining optical fiber, where each generated polarization state must be the same as the detected or analyzed [8]. We have used a

high-quality photonic crystal fiber as the calibration reference; however, it is not as good as required.

The Fig. 4 shows the Poincaré output spheres associated to each optical fiber. They represent how the incident Stokes vectors are mapped after their transmission through the optical fibers.

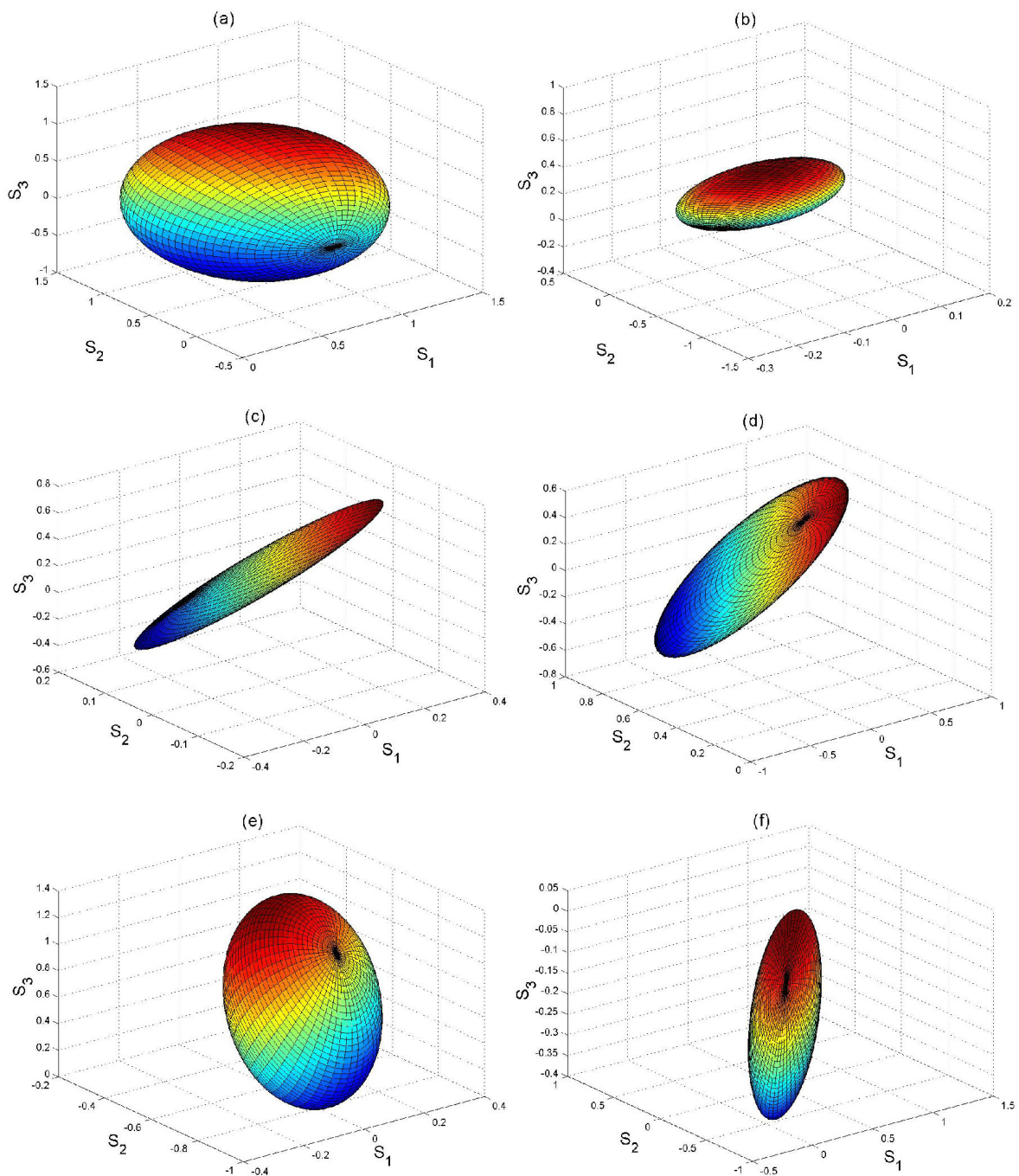


FIGURE 4. Poincaré output sphere associated to fibers a (Fig. 4.a), b (Fig. 4.b), c (Fig. 4.c), d, (Fig. 4.d), e (Fig. 4.e), and f (Fig. 4.f).

Observe the spherical shapes and sizes are lost progressively according the depolarization responses associated to each fiber is increased and that the depolarization depends strongly on the incident polarization state. This behavior is consistent with the results shown in Table II and in Fig. 3.

5. Conclusions

Fourteen polarimetric parameters and a graphical analysis have been performed for six different types of commercial

optical fibers, for a transmission wavelength of 1550 nm. All of them have been determined from the experimental Mueller matrix associated to each fiber studied. Results are consistent and show the performance of each optical fiber is directly related to its polarization properties, suggesting the fibers can be used not only as static elements, but also as versatile optical devices, depending on the incident polarization state employed. According to our results, the optical fiber FS-PM-6621 (named here as fiber *c*), presents the lowest value of PDL for this set of commercial fibers; in this sense, this fiber

can be used in modern fiber communication systems for long distances or in the construction of devices like optical couplers, pump diode pigtailed gratings, among many other applications. On the other hand, fiber *b* (Nufern's 980 nm, 980 HP), presents the highest value of PDL, which makes it a good candidate as a fiber inline linear polarizer due to its capability to polarize the transmitted light. Note the ESM-12-01 (fiber *a*), has the lowest depolarization and anisotropic depolarization degree, which means it has a lower and almost uniform birefringence and presents a high quality composition. We suggest this fiber be used in encrypted telecommunication systems. Even when we have determined these polarimetric characteristics at a single wavelength (1500 nm),

our main goal with this work has been to present a methodology able to be applied for any interested user according their own needs. An improvement to a reported method by our group has been presented for the data analysis.

Acknowledgments

O. J. Velarde-Escobar (16821) and K. M. Salas-Alcántara (241632) express their gratitude to CONACYT (México) for the scholarships received through their doctoral studies. This work has been done with the financial support of CONACYT-México (project 100361).

-
1. A. Ghatak, K. Thyagarajan, *An Introduction To Fiber Optics*, (Cambridge University Press, New York 1998).
 2. B. Culshaw and J. Dakin, Eds, *Optical Fiber Sensors: Systems and Applications*, Vol. II, (Artech House 1989).
 3. A. Mendez, *Specialty Optical Fibers in Biomedical Applications: Needs & Applications*, in Workshop on Specialty Optical Fibers and their Applications, (Optical Society of America 2013).
 4. Q. Wang, G. Farrell, T. Freir, G. Rajan, and P. Wang, *Opt. Lett.* **31** (2006) 1785-1787.
 5. E. Collett, *Polarized Light in fiber Optics*, The PolaWave Group (2003).
 6. X. Wang, P. Moraw, D. R. Reilly, J. B. Altepeter, and G. S. Kanter, *J. Lightwave Tech.* **31** (2013) 707-714.
 7. K. M. Salas-Alcántara, R. Espinosa-Luna, and I. Torres-Gómez, *Opt. Eng.* **51** (2012) 085005.
 8. K. M. Salas-Alcántara, R. Espinosa-Luna, I. Torres-Gómez, and Y. Barmenkov, *Appl. Opt.* **53** (2014) 269-277.
 9. N. Ghosh, M. F. G. Wood, and I. A. Vitkin, *J. Biomed. Opt.* **13** (2008) 044036.
 10. T. A. Eftimov, W. J. Bock, P. Mikulic, and J. Chen, *J. Lightwave Technol.* **27** (2009) 3759-3764.
 11. D. Godstein, *Polarized Light*, 2nd Ed., (Marcel Decker 2003).
 12. S.Y. Lu and R. A. Chipman, *J. Opt. Soc. Am. A* **13** (2006) 1106-1113.
 13. J. J. Gil and E. Bernabeu, *Opt. Acta* **32** (1985) 259-261.
 14. R. Espinosa-Luna and E. Bernabeu, *Opt. Commun.* **277** (2007) 256-258.
 15. R. Espinosa-Luna, G. Atondo-Rubio, S. Hinojosa-Ruiz, *Optik* **121** (2010) 1058-1068.